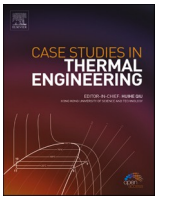
Case Studies in Thermal Engineering 28 (2021) 101489



Contents lists available at ScienceDirect

Case Studies in Thermal Engineering

journal homepage: www.elsevier.com/locate/csite



Comparative performance evaluation of the mechanical and adsorption hybrid cooling systems for the cascaded and the serial connected evaporators configurations

Muhsin Kiliç *, Mustafa Anjrini

Department of Mechanical Engineering, Engineering Faculty, Bursa Uludağ University, Bursa, Turkey

ARTICLE INFO

Keywords:
Adsorbents
Combined cooling system
Different configurations
Exergy
Performance

ABSTRACT

The goal of this study is to investigate comparatively the performance of an integrated cooling system comprised of an adsorption cooling cycle (ADC) and a vapor cooling cycle (VCC) with two different configurations, namely (cascaded and serial connected evaporators). The ADC chiller relies on the thermal compressor with two adsorption beds, which use three different adsorbents (RD silica gel, RD silica gel 2060, and silica gel- LiCl) and water (adsorbate) as a working pair separately. The thermal compressor operates by outside waste or solar-based thermal sources that have low-level temperatures below 100 °C. R152A was selected for the VCC chiller. This article pays particular attention to evaluating the ADC adsorbents and (ADC-VCC) connection configurations based on the first and second law of thermodynamics. The investigations have been implemented at different ADC evaporator temperatures. The effect of adsorption cycle time and ambient temperature on the overall coefficient of performance were also investigated and discussed for both configurations. Furthermore, the ADC and VCC coefficient of performances and the performance ratio (PR) were investigated at different ADC evaporator temperatures. The relation between the adsorbent mass and the cooling load was also discussed in this paper.

1. Introduction

Researchers have recently tried to discover new ways to reduce the massive consumption of energy. As the refrigeration systems consume a tremendous amount of energy, which is almost 40% of the produced power, new cooling techniques are under discovery to lessen that demand. Lately, adsorption refrigeration systems have attracted many researchers as this kind of technology can use waste heat, solar energy, and geothermal energy at low-grade temperatures to drive the system. Plenty of investigations have been done on the adsorption system using different working pairs and various layouts.

As the adsorption refrigeration systems employ waste heat or solar energy to meet the cooling effects, thermal compression is used in the adsorption chiller, which is the essential component of the system. The working pair (adsorbent/adsorbate) also offers various application choices that specify the equilibrium states of the adsorption/desorption process. Indeed, various sorption working pairs have been studied and experimented by several researchers, such as (activated carbon/methanol/ethanol, zeolite/water, silica gel/water/ammonia, etc.) [1–4]. Kilic [5] investigated the silica gel as an adsorbent with different refrigerants (adsorbates) like (R404A, water, R134A, Methanol) at a low-level temperature heat source almost (≤95 °C). Among the working pairs considered in that study,

* Corresponding author.
E-mail address: mkilic@uludag.edu.tr (M. Kiliç).

https://doi.org/10.1016/j.csite.2021.101489
Received 18 August 2021; Received in revised form 21 September 2021; Accepted 22 September 2021
Available online 25 September 2021
2214-157X/© 2021 The Authors. Published by Elsevier Ltd. This is an open access article under the CC BY-NC-ND license (http://creativecommons.org/licenses/by-nc-nd/4.0/).

Nomenclature

A	Area, [m^2]
a	Specific area, [m^2 /g]
COP	Coefficient of performance, [non-dimensional]
Cp	Specific heat, [J/kg.K]
D	Diameter of the solid sorbent grains, [m]
D_o	Pre-exponent constant, [m^2/s]
D_{po}	The diameter of adsorbent pore, [m]
E	Characteristic energy of the pairs considered in the bed, [kJ/kg]
E_a	the activation energy of the pairs considered in the bed, [kJ/kg]
h	Enthalpy, [kJ/kg]
h_{fg}	Vaporization enthalpy, [kJ/kg]
Δh_{ads}	Adsorption heat, [kJ/kg]
M	Mass, [kg]
n	Exponential constant, [−]
P	Pressure, [kPa]
P_s	Pressure at saturation conditions, [kPa]
PR	Performance ratio, [−]
$\dot{Q}$	Heat transfer rate, [kW]
r_p	Average radius of the solid sorbent particle, [m]
s	Entropy, [kJ/kg.K]
SCP	Specific cooling power; [W/kg]
T	Temperature, [°C]
ΔT_{lm}	Logarithmic mean temperature difference, [°C]
t	Time, [s]
U	Overall heat transfer coefficient, [W/m^2.°C]
V_{Po}	Volume of the pore in the adsorbent, [cc/g]
W	adsorption space uptake of the solid adsorbent, [m^3 /kg]
W_o	Limiting adsorption space uptake of the adsorbent, [m^3/kg]
X	Specific adsorbed mass of adsorbate, [kg/kg]
X_o	Limiting the specific adsorbed mass of adsorbate, [kg/kg]
Ɛ	Effectiveness, [−]

SUBSCRIPTS

ADC	Adsorption cooling cycle
Type A	Cascaded configuration, Fig. 1**a**
ad	Adsorption
amb	Ambient air
Type B	Serial connected evaporators configuration, Fig. 1**b**
bm	Bed material
cf	Cooling fluid
con	Condenser
des	Desorption
eva	Evaporator
eq	Equilibrium
elec	Electric
H	Hybrid
h	Hot
i	Isentropic
in	Inlet;
LDF	Linear driving force
liq	Liquid
max	Maximum
min	Minimum
out	Outlet;
SF	Second Fluid
SG	Silica gel
tot	Total
VCC	Vapor cooling cycle

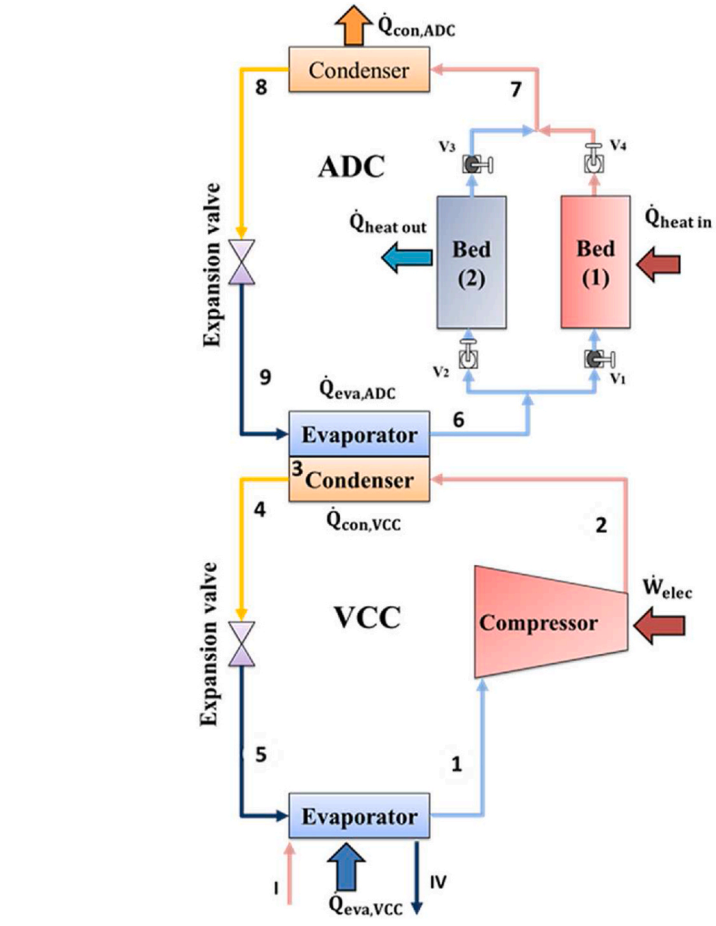
A,B,..F Thermodynamic points of the thermal compressor and ADC as in Fig. 2
1,2 …,10 Thermodynamic points of the proposed combined system as in Fig. 1
I,II,..IV Thermodynamic states of the second fluid connects the (ADC-VCC) evaporators in serial connected evaporators configuration related to Fig. 1 b

the highest performance indicators values were gained for the silica gel-water working pair with 0.63 and 0.329 kW/kg for the COP and SCP, respectively. Therefore, different types of silica gel were used in the adsorption chiller in the present study. Composite sorbents have also been recently investigated to be used in adsorption chillers. One of the inorganic salt such as (LiBr, LiCl, $CaCl_2$, $MgCl_2$, $MgSO_4$, etc.) is added to silica gel to form the composite adsorbent [6,7]. The inorganic salt is impregnated within the pores of the adsorbent (silica gel) to form the composite sorbent. Yet, the disadvantage of this sort of adsorbent is that some salt particles may stick on the adsorbent (silica gel) surface. Hence, the salt solution formed would fall and damage the chiller components [8].

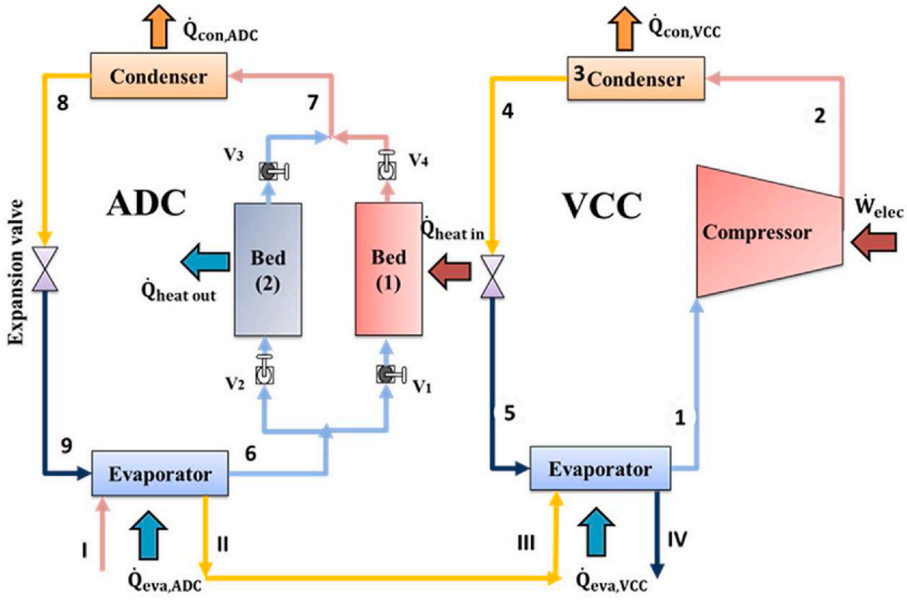
Conventional cooling systems directly or indirectly consume a considerable amount of energy and harm the ecological balance. New suggestions have been presented and experimented by integrating the traditional cooling cycle with new cooling technologies. One suggested layout combines the conventional vapor compression cooling system (VCC) with the adsorption cooling system (ADC) in one system. Vasta et al. [9] presented an article about testing a combined cooling system comprised of adsorption chiller and vapor compression chiller under actual working conditions to be used in air conditioning applications. Their results show that using a cascade cooling system allows saving energy by 50% compared to a conventional chiller alone. Uddin et al. [10] analytically investigated the performance of (ADC-VCC) combined cooling system using two different cycle layouts, namely cascade and sub-cooled types. They used activated carbon/ethanol as a working pair in the ADC unit. They utilized four different working fluids (R152a, R134a, R1234ze, and R1234yf) in the VCC unit. Their findings indicate that the energy savings by using the cascade connection can reach up to 19% compared to the conventional chiller, depending on the refrigerants selected in the VCC chiller. Kumar et al. [3] submitted an empirical analysis of mechanical - adsorption combined cooling system with activated carbon/CO_2 as a working pair. The investigation has been done by two configurations depending on the position of the mechanical compressor. The results indicate that the mechanical compressor compression power is lower when the mechanical compressor is in the low stage position. Additionally, the mass of carbon refrigerant requirement is higher when the mechanical compressor is in a low stage position compared to the other position. The authors indicated that the suggested system is appropriate for a few kilowatts loads. Palomba et al. [11] have investigated the efficient exploitation of renewables for adsorption-vapor compression combined cooling systems. The study examined three different layouts (parallel connection, series connection, and cascade connection). Silica gel/water was the working pair chosen for the adsorption chiller, whereas four different refrigerants (CO_2, R134a, R290, and R1270) were chosen in the vapor compression chiller. The study analyzed the capacity ratio, which is the ratio between the heat rejected from the vapor compression condenser and the heat absorbed into the evaporator of the ADC unit; the researchers found that the optimum value is close to one. The results also concluded that suitable refrigerant in VCC is the one that affects the volume and size of the overall combined system. Moreover, the results indicated that a shorter cycle time could be utilized when higher cooling power is required. Lychnos et al. [12,13] manufactured and tested a prototype of an adsorption-vapor compression combined cooling system. The activated carbon/R723 working pair was used in the adsorption chiller, while the R723 refrigerant was chosen in the vapor compression chiller. R723 is an ammonia mixture (60% Ammonia, 40% Dimethylether). The paper explained four configurations of the combined cooling systems using thermal and compression cycles. The experimental results pointed out that the parallel combined system can provide 6 kW of refrigeration capacity with both chillers (2 kW from the adsorption chiller at 80 °C driving temperature and 4 kW from the vapor mechanical chiller). Kilic et al. [14] also investigated the performance of combining the traditional chiller (VCC) and the adsorption chiller (ADC) by considering silica gel/water in the adsorption unit and five different kinds of refrigerants in the vapor compression unit, namely (R152A, R32, R1270, R410A, and R1234yf). The study also compared the VCC chiller working alone and integrated in terms of energy savings and performance. They found that R152A refrigerant gives the highest performance values, while R1234yf refrigerant gives the highest energy-saving values among the refrigerants considered. The results of their research also concluded that reducing the cycle time in adsorption chiller can lessen the adsorbent mass in the ADC thermal compressor.

In the literature, many investigations have been done on utilizing different layouts of the thermal compression (absorption-adsorption) chiller integrated with the conventional vapor mechanical chiller such as refs [15–17] for absorption-vapor compression combined cooling system and refs [10,11] for adsorption-vapor compression combined cooling system. Many functions have been observed using the different combined configurations, which depend on the application, whether to fragmentize the compression ratio or the cooling loads between the thermal and mechanical compression chillers, as an example.

The current study's objective is to present a comparative investigation of the performance in the combined cooling system consisting of ADC and VCC chillers. A mathematical model is used to accomplish the study objectives, which is suitably validated with the available empirical results in the previous studies. The comparative investigation has been carried out by utilizing several adsorbents (RD silica gel, RD silica gel 2060, and silica gel-LiCl) with water in the thermal compression chiller and employing R152A refrigerant in the mechanical compression chiller. This paper's other goal is to appraise the performance of two different (ADC-VCC) combined configurations, namely (cascaded connection and serial connected evaporators). Therefore, the current research findings allow us to notice the behavior of the proposed integrated cooling system using the different ADC working pairs and the hybridization of ADC and VCC units in two different configurations (cascaded connection and serial connected evaporators) at various ADC evaporator temperatures. The setting of ADC evaporator temperature relates to the VCC condenser temperature and other conditions that are also mentioned in this paper. This study also appraisals the connection between the adsorbent mass and the type of adsorbent at different ADC cooling loads that have not also been discussed in the previous researches. The effect of utilizing different adsorption cycle times



(a)



(b)

(caption on next page)

Fig. 1. The schematic diagram of two beds ADC system combined with VCC unit: (a) cascaded configuration (type A); (b) serial connected evaporators configuration (type B).

and ambient temperature on the performance of the two different configurations has also been plotted and discussed in this paper. Additionally, the electrical energy saving ratio, VCC performance ratio, and ADC performance ratio were also discussed as if there is no ADC and VCC unit hybridization under the same operating conditions.

2. Describing the (ADC-VCC) combined cooling system configurations

The presented combined cooling system consists of two chillers. Adsorption chiller (ADC) has four important components: the thermal compressor (adsorption bed), which is the vital part of this cycle, condenser, evaporator, and the expansion valve. The adsorption phenomenon is explained as the refrigerant (adsorbate) particles are settled down at the surface of the solid sorbent between the granular because of the strong attractive and electrostatic forces among the particles. Once the bed temperature is high, the solid sorbent releases the refrigerant (adsorbate) molecules and adsorbs them when its temperature is low. Thus, the function of the thermal compressor is to drive the refrigerant to the entire ADC system [18].

The vapor cooling cycle (VCC), on the other hand, has four main elements: vapor mechanical compressor, evaporator, expansion valve, and condenser. The proposed two cooling cycles (ADC and VCC) can be physically linked with different configurations. Two potential operating modes are presented: cascaded (type A) and serial connected evaporators (type B) configurations. Fig. 1 illustrates the two different combined system configurations shown in this article to be analyzed and compared.

In a cascaded configuration (Fig. 1a), the linkage of the two chillers occurs in the intermediate heat exchanger, which is the evaporator in the ADC chiller and the condenser in the VCC chiller. The difference between condensation and evaporation temperatures is about (5 °C) in this study. In this layout, the VCC chiller operates between the evaporation temperature required by the user and the intermediate temperature (VCC condenser temperature). In contrast, the ADC chiller works between the moderate temperature (ADC evaporator temperature) and the ADC condenser heat rejection temperature. Thus, the evaporator in ADC chiller provides the cooling effects to the condenser of the VCC chiller. Both cooling units supply cooling effects to the utilizer in the second layout (Fig. 1b). Both chillers operate between the user side temperature and rejection heat temperature. The total heat load is divided into two parts according to each cycle's working conditions in this configuration. Furthermore, this combination allows the ADC unit to cover the primary cooling load, while the VCC can be added to cover the peak load. As a result, a smaller size for both chillers is preferred.

As shown in Fig. 1 (a), the evaporator absorbs the heat from the refrigerated area in the VCC chiller and transmits it into the adsorption chiller. The heat exchanger at the middle (evaporator in the upper chiller and condenser in the bottom) takes all the rejection heat and completes the mission. In the ADC chiller, the refrigerant vapors enter the thermal compressor (adsorption bed), where the solid adsorbent adsorbed when connecting the bed to an outsource cooling fluid. Then, the adsorbate is desorbed from the thermal compressor when connecting the bed to the outsourcing heating fluid. The adsorbate vapor is pushed to the condenser, where it is cooled down by rejecting the heat to the ambient and condensed to be in a liquid stage. The refrigerant expands to the ADC evaporator pressure in the expansion valve. The refrigerant is vaporized in the ADC evaporator by absorbing the rejected heat from the condenser of the VCC chiller in the middle heat exchanger (ADC side). After the adsorption conditions are supplied in the thermal compressor, the refrigerant (adsorbate) vapors enter the thermal compressor to repeat the cooling cycle.

In the serial connected evaporators case (type B), Fig. 1 b, some of the cooling load that the user requires is accomplished by the ADC evaporator, while the VCC evaporator absorbs the remaining cooling load. A secondary fluid cycle that links the two chillers

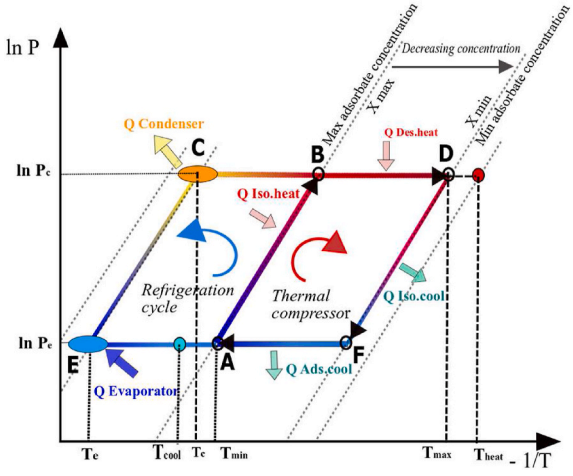


Fig. 2. Fundamental thermodynamic cycle for ADC unit [14].

enters the ADC evaporator to leave some of its heat in the ADC evaporator and exits at a temperature level higher than the ADC evaporator. Then, it enters the VCC evaporator to leave the rest of its heat and leaves at the temperature level determined by the user but higher than the VCC evaporator temperature level. It is noteworthy to refer that the temperature levels in both evaporators are different, which depends on each chiller's design conditions.

To comprehend the working concept of the thermal compressor, the four primary processes have been sectioned into isosteric heating (Fig. 2A-B), and isosteric cooling (Fig. 2 D-F) processes where mass changing is not observed. Adsorption (Fig. 2F-A) and desorption (Fig. 2B-D) processes where a variation of the refrigerant concentricity is noticed at a steady pressure. The adsorption cooling thermodynamic cycle represented in lnP −1/T diagram is given in Fig. 2. More details about the thermodynamic processes and the preliminary computations of the thermodynamic states in the thermal compressor can be found in Refs. [5,14,19].

Various sorption beds (2, 4, or 6) can be utilized in the adsorption chiller to supply persistent cooling effects. By implementing the two-bed case, one of the sorption beds is exposed to a heat source with a high temperature to desorb the refrigerant (adsorbate). In contrast, the other sorption bed is exposed to a cold source with a low temperature (close to the ambient temperature) to adsorb the refrigerant. The mission of every sorption heat exchanger is alternated in the second cooling period. Thus, we acquire persistent operating conditions of the refrigerating effect.

Before analyzing the adsorption chiller, several presumptions have been suggested in the previous studies. Sharafian et al. [20] grouped the mathematical correlations into three classifications (Lumped-body model, Geometry – dependent models, and Analytical model). The present article concentrates on the lumped–body model, where the researchers also collected them into three sub-groups (dynamic modeling, fully dynamic modeling, and quasi-steady-state). The fully dynamic model demands plenty of inputs. However, it can estimate the rate of adsorbate uptake, coefficient of performance, specific cooling power, and requisite time with credible precision. Further information about the other kinds can be investigated in Ref. [20].

3. The mathematical model for (ADC-VCC) integrated cooling system

The mathematical model is explained under three subheadings named as "ADC mathematical model", "VDC mathematical model" and "System performance indicators".

3.1. ADC mathematical model

While computing the proposed chiller's performance indicators, it is essential to indicate that the primary measurable factors are connected to adsorption heat and isotherms of the working pair (adsorbent/adsorbate) in the ADC chiller. Several parameters are utilized to compute the ADC performance. Undoubtedly, there are many hypotheses that must be taken into account for the investigation; the essential ones are as the following:

1 During the adsorption and desorption processes, the pressure losses are negligible.
2 During the isosteric cooling and isosteric heating modes, there are no mass flows.
3 The pressure losses in the evaporator, condenser and thermal compressor are overlooked.
4 The ADC chiller is entirely insulated.
5 The adsorption kinetics is related to the variation between the uptake at the equilibrium conditions and the momentary uptake.

3.1.1. Adsorption isotherm

Adsorption isotherm presents the refrigerant amount accumulated between the granular of the sorption bed in balance situations. Many correlations have been used for several kinds of adsorbent materials that explain the adsorption isotherms. It has, however, become a widespread way to utilize Dubinin-Astakhov (D-A) model for computing the value of refrigerant uptake on the solid sorbent which is related to temperature and pressure in the thermal compressor [21,22]. The expression of Dubinin-Astakhov (D-A) model is given in Eq. (1):

$$W = W_o . Exp\left\{ \left[\frac{RT}{E} \, ln \left(\frac{P_s}{P} \right) \right]^n \right\} \tag{1}$$

The parameter explanation of Eq. (1) and their values for the adsorbate (water) used in this investigation can be found in our previous article Kilic et al. [14].

3.1.2. Adsorption kinetics

The differences of the refrigerant concentration in the solid sorbent according to the time can be defined by the (LDF) model [23, 24], where the resistance of mass diffusion in the sorption material is taken into account. Adsorption kinetics formulation can be written as:

$$\frac{dX}{dt} = \frac{15 \, .D_o}{r_p^2} \exp\left(-\frac{E_a}{R.T} \right) \left(X_{eq} - X \right) \rightarrow X_{(t)} \Big/ X_{eq} = 1 - \exp\left(-\frac{15.D_o}{r_p^2} \exp\left(-\frac{E_a}{R.T} \right) t \right) \tag{2}$$

where X_{eq} is the balance concentricity at a specified pressure along with temperature.

The values of the solid materials traits utilized in this research can be obtained from Table 1.

3.1.3. Energy equilibrium equations

The correlation of energy equilibrium in the sorption bed (adsorbent) for the adsorption and pre-cooling operations are written as the following equation.

$$\dot{Q}_{cool,ADC} = m_{ads}\frac{dX_{ad,f}}{dt}\left(\Delta h_{ads} + \gamma h_{eva,out} - h_{ad,f}\right) + \frac{dm_{bed,v}}{dt}\left(\gamma h_{bed,in} - h_{bed,v}\right)$$

$$-\left[m_{bm}c_{p,bm} + m_{ads}c_{p,ads}\right]\frac{dT_{bed}}{dt} - \left(m_{ads}X_{ad,f}\right)\frac{dh_{ad,f}}{dt} - \left(m_{bed,v}\right)\frac{dh_{bed,v}}{dt} \quad (3)$$

Where the value of $\gamma$is equal to zero in the pre-cooling process and to one in the adsorption process.

The energy equilibrium formulation in the adsorbent according to the desorption and pre-heating processes can be written as the following equation.

$$\dot{Q}_{heat,ADC} = \left[m_{bm}c_{p,bm} + m_{ads}c_{p,ads}\right]\frac{dT_{bed}}{dt} + \left(m_{ads}X_{ad,f}\right)\frac{dh_{ad,f}}{dt} + \left(m_{bed,v}\right)\frac{dh_{bed,v}}{dt}$$

$$+m_{ads}\frac{dX_{ad,f}}{dt}\left(\Delta h_{ads} + \gamma h_{con,in} - h_{ad,f}\right) - \frac{dm_{bed,v}}{dt}\left(\gamma h_{bed,out} - h_{bed,v}\right) \quad (4)$$

Where the value of γ is equal to zero in the pre-heating process and to one in the desorption process.

Δh_{ads} is the adsorption enthalpy that can be computed by the equation suggested by El- Sharkawy et al. [25] that expressed as Eq. (5):

$$\Delta h_{\mathrm{ads}} = h_{\mathrm{fg}} + (E)\left[ln\left(\frac{W_o}{w}\right)\right]^{1/n} + (E.T.\Omega)\left[ln\left(\frac{W_o}{w}\right)\right]^{(1-n)/n} \quad (5)$$

3.1.4. Mass equilibrium equations

The refrigerant amount in the adsorbent can be taken at any instant from the following expression.

$$m_{bed,f} = m_{ads}X_{ad,f} + m_{bed,v} \quad (6)$$

Where the mass transfer rate from the evaporator to the sorption bed (adsorbent) in the adsorption mode might be expressed in Eqs. (7) and (8).

$$\frac{dm_{bed,f}}{dt} = m_{ads}\frac{dX_{ad,f}}{dt} + \frac{dm_{bed,v}}{dt} \quad (7)$$

$$\frac{dm_{eva,out}}{dt} = \frac{dm_{bed,in}}{dt} = \frac{dM_{bed,f}}{dt} \quad (8)$$

Likewise, the mass transfer rate from the sorption bed (adsorbent) to the condenser during the desorption mode might be expressed as Eqs. (7) and (9).

$$\frac{dm_{con,in}}{dt} = \frac{dm_{bed,out}}{dt} = \frac{dM_{bed,f}}{dt} \quad (9)$$

Table 1
Values of the parameters used in the present study for the three types of adsorbent and water [5,8,23].

Property	RD silica gel	RD silica gel 2060	silica gel-LiCl
Chemical formula	SiO_2.n(H_2O)	SiO_2.n(H_2O)	SiO_2.n(H_2O) + LiCl
D (mm)	0.8–0.89	0.5–0.59	0.5–1
a (m^2/g)	827.5	686.3	300
V_{Po}(cc/g)	0.462	0.335	1
D_{Po} (nm)	3.24	3.19	15
Inorganic salt content %	0	0	20
C_P (kJ/kg.K)	0.92	0.92	0.85
E (kJ/kg)	192.29	242.79	270.4
n	1.35	1.35	1.604
D_O (m^2/s)	2.8 E^{-4}	2.8 E^{-4}	2.54 E^{-4}
E_a (kJ/kg)	2247.5	2247.5	2020
r_P (m)	$4E^{-4}$	2.9 E^{-4}	4.75 E^{-4}
X_o(kg_{ref}/kg_{ads})	0.48	0.38	0.489

The cycling mass of the refrigerant might be calculated using Eq. (10) or Eq. (11). However, The non-cycling mass of the refrigerant in the ADC unit might be calculated using Eq. (12) as the following.

$$M_{cyc,ADC} = \int_{des} \frac{dm_{con,in}}{dt} dt = \int_{ads} \frac{dm_{eva,out}}{dt} dt \tag{10}$$

$$M_{cyc,ADC} = m_{ads}(X_{max} - X_{min}) + V_{bed,void}\left(\rho_{v,max} - \rho_{v,min}\right) \tag{11}$$

$$M_{ncyc,ADC} = m_{ads}X_{min} + V_{bed,void}\rho_v(P_{con}, T_{max}) \tag{12}$$

Where the void volume is represented by $V_{bed,\ void}$ that is used by the refrigerant in the vapor stage in the adsorbent. $\rho_{v,max}$ shows the maximum vapor density, the maximum bed temperature (T_{max}), and at the condenser pressure (P_{con}); $\rho_{v,min}$ represents the minimum vapor density at the minimum bed temperature (T_{min}) and the evaporator pressure (P_{eva}). Finally, the overall mass of the adsorbate implemented in the ADC is computed from the following expression.

$$M_{tf,ADC} = M_{cyc,ACC} + M_{ncyc,ADC} \tag{13}$$

3.1.5. ADC system performance indicators

The ADC performance indicators can be expressed by the coefficient of performance (COP_{ADC}) and the specific cooling power (SCP) in $W/kg_{adsorbent}$. These two indicators are the primary information for the ADC technical features. The COP_{ADC} and SCP values can be computed via Eq. (14) and Eq. (15), respectively.

$$COP_{ADC} = \frac{Q_{eva,ADC}}{Q_{heat,ACC}} \tag{14}$$

$$SCP = \frac{Q_{eva,ADC}}{t_{cycle}M_s} \tag{15}$$

The heat load ($Q_{heat,ADC}$) and the cooling capacity ($Q_{eva,ADC}$) of the ADC system in a cycle can be computed by Eq. (16) and Eq. (17), respectively.

$$Q_{heat,ADC} = \oint_0^{t_{cycle}} \dot{Q}_{heat,ADC} dt \tag{16}$$

$$Q_{eva,ADC} = \oint_0^{t_{cycle}} \frac{dm_{eva,out}}{dt}(h_6 - h_9) dt \tag{17}$$

It is noteworthy to mention that the consumptions of the electrical power in cooling, heating, and chilled fluids pumps or even fans are comparatively little. Thus, it can be omitted.

3.2. VCC mathematical model

The thermodynamic model of the VCC in this investigation depends on a basic one-stage cooling cycle. Fig. 1 clarifies the main

Table 2
Essential modes and mathematical correlations related to VCC chiller.

Component	Conditions and Correlations	Component	Conditions and Correlations
Evaporator	$T_1 = T_{eva} + 5$	Condensers	$P_2 = P_3 = P_4$
	$P_1 = f(T_1 = T_{eva},\ q = 1) = P_{eva}$		
	$h_1 = f(T_1\ P_1)$		$T_3 = T_{Con,VCC}$, $h_3 = f(P_3 q = 0)$, $S_3 = f(P_3 q = 0)$
	$S_1 = f(T_1,\ P_1)$		
	$\dot{Q}_{eva,VCC} = \dot{m}(h_1 - h_5)$ (18)		$T_4 = T_3 - 4$
Mechanical Compressor	$P_2 = P_{con}$		$h_4 = f(P_4\ T_4)$, $S_4 = f(P_4\ T_4)$
	$S_2 = S_1$		$\dot{Q}_{con} = \dot{m}(h_2 - h_4)$ *(20)*
	$h_{2s} = f(P_2, S_2 = S_1)$		
	$T_2 = f(P_2, S_2)$		
	$\eta_{elec} = 0.90$, $\eta_i = 0.80$	Expansion valve	$P_5 = P_1 = P_{eva}$
	$h_2 = (h_{2s} - h_1)/\eta_i + h_1$		$h_5 = h_4$
	$\dot{W}_{elec} = \frac{\dot{m}(h_2 - h_1)}{\eta_{ele}}$ (19)		$S_5 = f(P_5,\ h_5)$

elements of the VCC unit. Table 2 illustrates the mathematical computations and thermodynamic states of the vapor compression chiller. However, before the modeling, many hypotheses should be considered through the calculations as the following:

1 The VCC chiller runs under steady-state operation mode.
2 The differences in potential and kinetic energies are neglected.
3 The process in the expansion valve is isenthalpic.
4 There are neither Pressure drops nor heat losses in the VCC system.
5 Mass flow within the VCC unit is stable. $\dot{m}_1 = \dot{m}_2 = \dot{m}_3 = \dot{m}_4 = \dot{m}$

3.3. System performance indicators

The refrigerator's effectiveness is defined as the coefficient of performance. The objective of the cooling units is to withdraw an amount of heat $\dot{Q}_{eva}$ from the refrigerated materials or conditioned fluid are through consuming electrical power $\dot{W}_{elec}$. The coefficient of performance in the VCC unit is given by Eq. (21):

$$COP_{VCC} = \dot{Q}_{eva,\ VCC} \Big/ \dot{W}_{elec} \tag{21}$$

In this kind of combined chillers, the amount of rejected heat transmitted from the VCC condenser to the ADC evaporator (middle heat exchanger) (Fig. 1a) should be considered in a careful way. The absorbed heat in the evaporator of ADC must be equal to that released from the condenser of the VCC unit. Thus, while designing the (ADC-VCC) hybrid cooling system, the energy equilibrium equation must be satisfied with the cascaded configuration as to the following expression:

$$\dot{Q}_{eva,ADC} = \dot{Q}_{con,VCC} \tag{22}$$

The cooling load in the cascaded connection is ($\dot{Q}_{eva,\ tot} = \dot{Q}_{eva,\ VCC}$). In contrast, the cooling load in the serial connected evaporators configuration, Fig. 1b, is divided according to each chiller's operating conditions. Some assumptions have been made to calculate the cooling heat as the following: $T_I = T_{sf}$, $T_{II} = T_{eva,ADC} + 2$, $T_{III} = T_{II}$, $T_{IV} = T_1 + 3$. Thus, the total cooling load in the serial connected evaporators configuration can be computed by Eq. (23):

$$\dot{Q}_{eva,\ tot} = \dot{Q}_{eva,ADC} + \dot{Q}_{eva,VCC} \tag{23}$$

$$\dot{Q}_{eva,ADC,b} = \dot{m}_{SF}.Cp_{SF}\ (T_I - T_{II}) = (UA)_{eva,ADC,b}.(\Delta T_{lm})_{eva,ADC} \tag{24}$$

$$\dot{Q}_{eva,VCC,b} = \dot{m}_{SF}.Cp_{SF}\ (T_{III} - T_{IV}) = (UA)_{eva,VCC,b}\ (\Delta T_{lm})_{eva,VCC,b} \tag{25}$$

where

$$(\Delta T_{lm})_{eva,VCC,b} = \frac{(T_{III} - T_{eva,VCC}) - (T_{IV} - T_1)}{\ln\left(\frac{T_{III} - T_{eva,VCC}}{T_{IV} - T_1}\right)} \tag{26}$$

$$(\Delta T_{lm})_{eva,ADC,b} = \frac{(T_I - T_{eva,ADC}) - (T_{II} - T_{eva,ADC})}{\ln\left(\frac{T_I - T_{eva,ADC}}{T_{II} - T_{eva,ADC}}\right)} \tag{27}$$

Similarly, for the series connection:'

$$\dot{Q}_{eva,VCC,a} = \dot{m}_{SF}.Cp_{SF}\ (T_{III} - T_{IV}) = (UA)_{eva,VCC,a}\ (\Delta T_{lm})_{eva,VCC,a} \tag{28}$$

where

$$(\Delta T_{lm})_{eva,VCC,a} = \frac{(T_I - T_{eva,VCC}) - (T_{IV} - T_1)}{\ln\left(\frac{T_I - T_{eva,VCC}}{T_{IV} - T_1}\right)} \tag{29}$$

Thus, the effectiveness value for the ADC and VCC evaporators according to the two configurations considered cascaded (a) and serial connected evaporators configuration (b) can be expressed as:

$$\varepsilon_{eva,ADC,b} = 1 - e^{-(UA)_{eva,ADC,b} \Big/ \dot{m}_{SF}.Cp_{SF}} \tag{30}$$

$$\varepsilon_{eva,VCC,b} = 1 - e^{-(UA)_{eva,VCC,b} \Big/ \dot{m}_{SF}.Cp_{SF}} \tag{31}$$

$$\varepsilon_{eva,VCC,a} = 1 - e^{-(UA)_{eva,VCC,a} \Big/ \dot{m}_{SF}.Cp_{SF}} \tag{32}$$

It is noteworthy to mention that the second fluid used in the pipes that links the (ADC-VCC) evaporators in the serial connected evaporators configuration and the VCC evaporator in the cascaded configuration is water.

To compare the performance of the proposed combined cooling system, it is possible to utilize the hybrid coefficient of performance COP_H of the whole integrated system, which can be known as the proportion between the total refrigerating power provided whether for cascaded (type A) or serial connected evaporators (type B) layouts and the entire energy rate provided to the combined cooling system:

$$COP_H = \dot{Q}_{eva,\ tot} \Big/ \left(\dot{Q}_{heat,ADC} + \dot{W}_{elec} \right) \tag{33}$$

The denominator, however, contains the combination of VCC electric power input and ADC thermal input values, which gives incorrect values. Therefore, there is an advantage of utilizing the exergy concept to avoid this issue. We can apply the exergy concept by turning the heat amounts in both the VCC evaporator and energy input in ADC to their exergy values. The surrounding temperature is the reference temperature utilized in the exergy expression. Thus, the hybrid cooling system performance has become like the following expression for the cascaded configurations illustrated in Fig. 1 a:

$$COP_{EXE,H} = \left[\dot{Q}_{eva,VCC} \left(1 - \frac{T_{eva,VCC}}{T_{amb}} \right) \right] \Big/ \left[\dot{W}_{elec} + \dot{Q}_{heat,ADC} \left(1 - \frac{T_{amb}}{T_{h,ADC}} \right) \right] \tag{34}$$

The performance of the hybrid cooling system for the serial connected evaporators configuration illustrated in Fig. 1.b can be expressed as the following equation:

$$COP_{EXE,H} = \left[\dot{Q}_{eva,VCC} \left(1 - \frac{T_{eva,VCC}}{T_{amb}} \right) + \dot{Q}_{eva,ACC} \left(1 - \frac{T_{eva,ADC}}{T_{amb}} \right) \right] \Big/ \left[\dot{W}_{elec} + \dot{Q}_{heat,ACC} \left(1 - \frac{T_{amb}}{T_{h,ADC}} \right) \right] \tag{35}$$

4. Evaluating the performance and electrical energy saving ratios

Analyzing the cooling system performances and electrical energy saving ratio in this integration cooling system compared to operating each system alone gives us a clue about the advantages and disadvantages of connecting the two chillers in cascaded and serial connected evaporators configurations. The electrical energy saving ratio (EESR) when the VCC operates with the ADC unit and when it works alone can be expressed in Eq. (36). Additionally, the VCC performance ratio and ADC performance ratio as each cooling system operates in one system or individually at the same running conditions can be expressed in Eq. (37) and Eq. (38), respectively.

$$EESR = \left[\left(\dot{W}_{elec,VCC} - \dot{W}_{elec,H} \right) \Big/ \dot{W}_{elec,VCC} \right] * 100 \tag{36}$$

$$PR_{VCC} = COP_{VCC,H} \big/ COP_{VCC} \tag{37}$$

$$PR_{ADC} = COP_{ADC,H} \big/ COP_{ADC} \tag{38}$$

5. Calculations procedure and validation of the mathematical model

The ADC mathematical codes are formed in the RAD studio 10 environment utilizing Delphi 10 program language. The thermophysical fluid properties considered are used as actual fluid properties by utilizing the CoolProp library formed in the C++ platform, which can compute properties for more than 100 various fluids with pretty good accuracy. More details about the CoolProp library might be found in Bell et al. [26]. Besides that, the amount of adsorption heat is computed as a function of temperature, concentration, and pressure. The above-mentioned equations are solved by an iterative method. In contrast, the VCC mathematical codes are written in the Engineering Equation solver (EES).

Various studies have already been submitted that investigate the adsorption chillers using silica gel/water as a working pair. Di et al. [27] as well as Vodianitskaia et al. [18] implemented an experiential investigation by considering silica gel-water as a working pair. The results in these investigations are utilized to prove the validity of the current model for the ADC unit. The calculations are executed according to the operating conditions and parameters specified in the mentioned reference papers. Di et al. [27] illustrated that the heat capacity of the thermal compressor material also influences on the system performance indicators. Therefore, they proposed a thermal capacity ratio expressed as the following equation:

$$R_m = (m.c_p)_{bm} / (m.c_p)_{ads} \tag{39}$$

When the value of R_m increases, further cooling and heating effects are needed for the thermal compressor, this leads to a reduction in the coefficient of performance. R_m is considered as 3 in their investigations. Our previous paper [14] reports the validation between the currently calculated outcomes and the data of Di et al. [27] according to various heat inlet temperatures. The predicted values of SCP and COP were in good compatibility with the experiential measurements of Di et al. [27].

More lately, Vodianitskaia et al. [18] conducted an experiential investigation on the adsorption cooling system employing silica gel/water as a working pair. In their research, temperature, pressure, and refrigerant flow measurements were also implemented for two different types of solid sorbent granular volumes to match the resulting performance and dynamics. Our previous paper [14] also shows the comparisons between the current data and the results of Vodianitskaia et al. [18] with various heating inlet temperatures within 65–95 °C, where the maximum deviations are 6.9% and 3.8% for SCP and COP, respectively.

In the literature, few studies have been implemented on the (ADC-VCC) combined cooling system. Vasta et al. [9] carried out an experiential investigation on (ADC-VCC) combined cycles by using a silica gel/water and changing both the heat source temperature and surrounding temperature. VCC chiller employing R410A working fluid was utilized in their empirical rig. Our paper [14] reports the comparisons between the current calculations and the empirical findings of Vasta et al. [9] according to various surrounding air temperatures. The same operating conditions and parameters are considered in the present computations. Some thermodynamical and physical parameters have also been used from Refs. [5,21] to investigate system performance behavior.

As a result, the current mathematical model is validated in a suitable manner. The present mathematical model that has been validated in our previous paper [14] can be considered dependable and robust; the validated mathematical code can be confidently utilized in additional studies.

6. Evaluation of the VCC refrigerants

Using the correct working fluid in the mechanical chiller is considered an essential element in evaluating system performance. Besides that, the ecological issues of the selected VCC working fluid should also be considered. In actuality, several VCC refrigerants act differently in the cooling system. A proper refrigerant is, undoubtedly, the one that gives the highest performance in the whole system and has minimum or no environmental effects. The various sorts of working fluids can be grouped into chemical collections and generations. The mutual points that should be considered are the global warming potential (GWP), ozone depletion potential (ODP), flammability, and toxicity. Further information about the kinds of working fluids and their groups can be obtained from Bolaji et al. [28].

In the (ADC-VCC) integrated cooling system, three types of adsorbents (RD silica gel, RD silica gel 2060, and silica gel-LiCl) were considered with water as the refrigerant in the ADC chiller. R152A was employed in the VCC chiller as it gives the best system performance values among the considered refrigerants in our previous paper [14].

7. Result and discussion

The current paper aims to mainly compare the performance of the (ADC-VCC) combined cooling system. The comparative work is implemented by using two configurations (cascaded configuration (type A) and serial connected evaporators configuration (type B)). The research was conducted by considering the typical boundaries of refrigeration and air conditioning applications. The difference between the condensing temperature in the VCC chiller and the evaporating temperature in the ADC chiller is kept constant at ($\Delta T = 5$ °C) in the cascaded configuration. The cooling fluid works to cool down the ADC condenser as well as the solid sorbents through the adsorption and pre-cooling operations, where its inlet temperature is kept constant at 30 °C. The surrounding temperature is considered at 40 °C. The heating inlet temperature to the thermal compressor during the pre-heating and desorption processes remains stable at 95 °C. Even though the adsorption chiller's cycle time differs according to the adsorbent types utilized, it is assumed to be constant for all adsorbents considered in this paper. Table 3 presents the operating conditions and the parameters used in the current research.

Other parameter settings of the minimum and maximum temperatures are used as the following: $T_D = T_h - 5$ °C; $T_A = T_{cf} + 2$ °C.

The results in Fig. 3 state the amount of the cooling load absorbed in the ADC evaporator ($\dot{Q}_{eva,ADC}$) and VCC evaporator ($\dot{Q}_{eva,VCC}$) in the serial connected evaporators configuration (type B) with respect to the ADC evaporator temperature (T_{eva}) as the total cooling load in this research is kept constant as 10 kW. It is evident from the results that as the ADC evaporator temperature increases, the

Table 3
Parameters and working conditions which are utilized in the current research.

Mass of solid sorbent (adsorbent)	$m_{ads} = 44$ [kg]
Heating inlet temperature	$T_h = 95$ [°C]
Cooling inlet temperature	$T_{cool} = 30$ [°C]
ADC evaporation temperature	$T_{eva,ADC} = 10$ to 20 [°C]
ADC condensing temperature	$T_{con,ADC} = 45$ [°C]
Ambient temperature	$T_{amb} = 40$ [°C]
VCC condenser temperature (series connection)	$T_{con,VCC,a} = 15$ to 25 [°C]
VCC evaporation temperature	$T_{eva,VCC} = -5$ [°C]
Secondary fluid inlet temperature	$T_{SF} = 25$ [°C]
Total cooling load	$\dot{Q}_{tot} = 10$ [kW]
Heat capacity ratio	$R_m = 1.5$
Desorption/adsorption time	500 [s]
Pre-heating/pre-cooling time	50 [s]
ADC Cycle time	1100 [s]

cooling load in the ADC evaporator reduces while it increases in the VCC evaporator according to the operating conditions considered.

Fig. 4 states the amount of heat that the ADC system required to accomplish the adsorption cycle at different ADC evaporator temperatures according to the two different configurations. The results illustrate different heat transfer rate values by using the three different adsorbents due to the various physical and thermophysical properties among the adsorbents considered in this study, according to Table 1. The outcomes also reveal that the composite adsorbent (silica gel-LiCl) needs lower heat rates than the other adsorbents considered in the ADC chiller. It is clear that as the $T_{eva,ADC}$ increases the $\dot{Q}_{heat,ADC}$ gradually decreases. This behavior is due to a lower temperature difference between the evaporator and the condenser in the adsorption chiller as the ADC evaporator temperature increases. In contrast, the reduction in the amount of heat $\dot{Q}_{heat,ADC}$ required to the adsorption chiller in the type B configuration (Fig. 1b) is more than in the cascaded configuration (type A). Indeed, in the serial connected evaporators configuration, as the ADC evaporator temperature increases, the cooling load dramatically decreases $\dot{Q}_{eva,ADC}$ (Fig. 3); thus, the requisite heat to the adsorption chiller remarkably decreases. The highest $\dot{Q}_{heat,ADC}$ obtained is 22.2 kW at ($T_{eva,ADC} = 10\ ^{\circ}C$) for RD silica gel 2060 according to the (VCC-ADC) cascaded configuration, while the lowest $\dot{Q}_{heat,ADC}$ obtained is 7 kW at ($T_{eva,ADC} = 20\ ^{\circ}C$) for silica gel-LiCl at the same operating conditions according to the serial connected evaporators configuration. It is noticeable from Fig. 4 that RD silica gel 2060 consumes more amount of heat among the adsorbents considered for cascaded and serial connected evaporators configurations. Additionally, the reduction ratios in the heat transfer rate by increasing the ADC evaporator temperature from 10 °C to 20 °C are 9% and 52.4% for cascaded and serial connected evaporators configurations, respectively, which are almost the same for all the adsorbents considered.

Fig. 5 shows the comparison results of the proposed hybrid cooling system performance (cascaded (a) and serial connected evaporators (b)) between the different adsorbents considered in this paper at different ADC evaporator temperatures. It is clear from the results that elevating the ADC evaporator temperature $T_{eva,ADC}$ drives to a slight increase in the hybrid cooling system's coefficient of performance for the cascaded layout (a). Rising the ADC evaporator temperature drives to a decline in the amount of thermal energy $\dot{Q}_{heat,ADC}$. As we have previously mentioned that the temperature difference between ADC evaporator and VCC condenser is kept constant at ($\Delta T = 5\ ^{\circ}C$); thus, increasing the ADC evaporator and the VCC condenser temperatures result in an elevation in the electrical energy input to the mechanical compressor $\dot{W}_{elec}$, this leads to a slight increase in the performance values for the cascaded configuration (Fig. 1a). In contrast, it is evident from Fig. 5 that according to the serial connected evaporators configuration, increasing the ADC evaporator temperature $T_{eva,ADC}$ results in a considerable increase in the hybrid cooling system's coefficient of performance COP_H. According to the results in Fig. 4, elevating the ADC evaporator temperature results in a noticeable reduction in the heat energy $\dot{Q}_{heat,ADC}$. Therefore, the increase in the system performance values appears as illustrated in Fig. 5. The results also indicate that the composite adsorbent provides the highest system performance values COP_H as it consumes lower heat inputs $\dot{Q}_{heat,ADC}$ than the others considered in this paper. The highest hybrid cooling system performance reached 1.03 and 0.47 for the serial connected evaporators and the cascaded configurations. Additionally, the increasing ratios in the hybrid cooling system by increasing the ADC evaporator temperature from 10 °C to 20 °C are 3.4% and 66% for the cascaded and serial connected evaporators configurations, respectively, which are almost the same for all the adsorbents considered in this research.

Fig. 6(a) shows the overall system performance $COP_{EXE,H}$ using the exergy concept for different ADC evaporator temperatures employing various adsorbents in the ADC unit of the (VCC-ADC) cascaded configuration. It is noteworthy to indicate that the difference between the condensation temperature in VCC and evaporation temperature in ADC is kept constant ($\Delta T = 5\ ^{\circ}C$) for the cascaded configuration. The results show that employing the composite adsorbent (silica gel-LiCl) gives the highest performance values among the others considered. This behavior is because the composite adsorbent requires lower heat inputs to accomplish the desorption process than the other adsorbents considered, as shown in Fig. 4, leading to higher system performance values. In addition to that, it is

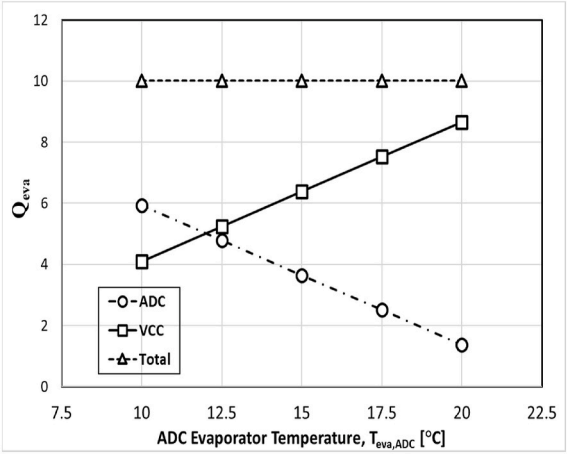


Fig. 3. Comparisons of $\dot{Q}_{eva}$ with respect to ADC evaporator temperature for serial connected evaporators configuration (Type B).

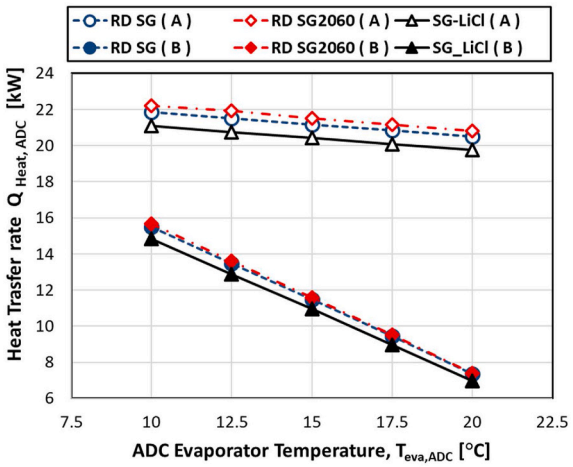


Fig. 4. Comparisons of $\dot{Q}_{heat,ADC}$ with respect to ADC evaporator temperature for the different adsorbents in ADC and the two system layouts (cascaded (type A) and serial connected evaporators (type B)).

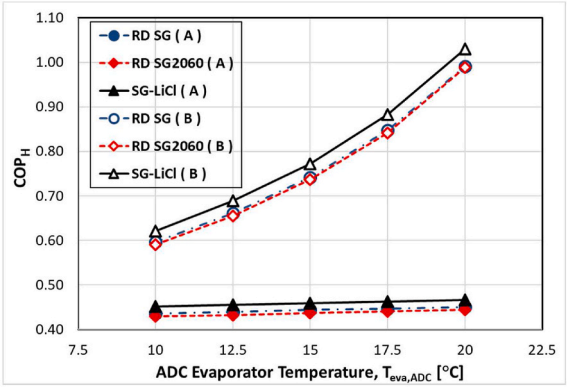
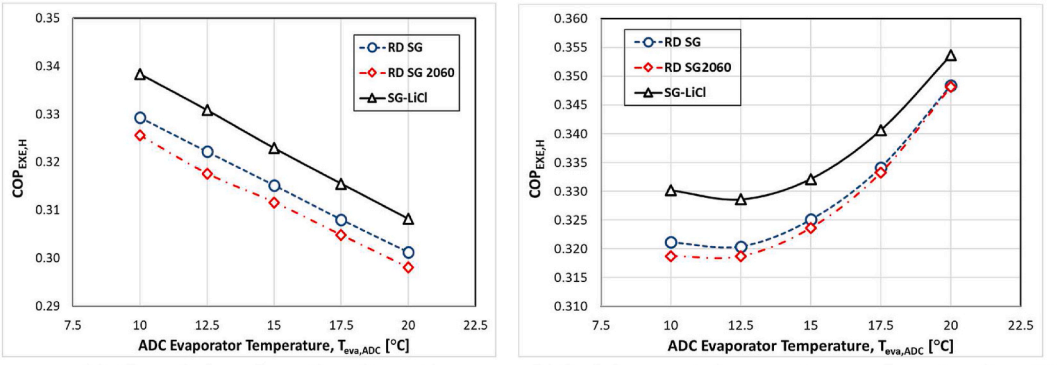


Fig. 5. Comparisons of COP_H with respect to ADC evaporator temperature for different adsorbents in ADC and (cascaded (type A) and serial connected evaporators (type B)) configurations.



(a) Cascaded configuration (type A) (b) Serial connected evaporators configuration (type B)

Fig. 6. Comparisons of $COP_{EXE,H}$ with respect to ADC evaporator temperature employing different adsorbents for cascaded configuration (a) and serial connected evaporators configuration.

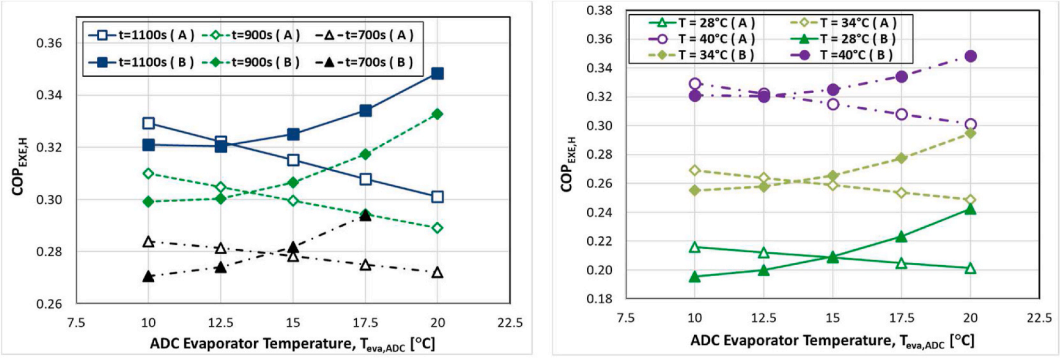
evident from Fig. 6 that the overall system performance value decreases as the $T_{eva.ADC}$ increases. Indeed, as the evaporator temperature in ADC and condenser temperature in VCC increase, the work input to the mechanical compressor also increases; thus, lower performance values were obtained. The highest and lowest performance values are 0.338 and 0.298 for silica gel-LiCl and RD silica gel

2060 at the lowest and highest ADC evaporator temperature considered in this study, respectively. Additionally, the reduction ratios in the overall combined system performance $COP_{EXE,H}$ by increasing the ADC temperature from 10 °C to 20 °C in the series configuration are almost 9.70%, 9.40%, and 9.74% for RD silica gel, RD silica gel 2060, silica gel-LiCl, respectively.

Fig. 6(b) shows the connection between the ADC evaporator temperature and the combined cooling system performance according to the serial connected evaporators configuration (Fig. 1b). As shown in (Fig. 1b), the two chillers are linked in serial. The total cooling load is divided into two parts; the ADC chiller accomplishes the first part while the VCC chiller completes the remaining amount successively. As the evaporator temperature changes, the ADC cooling load also changes; thus, the VCC cooling load changes. Eq. (35) is used to compute the $COP_{EXE,H}$ for the combined cooling system according to the serial connected evaporators layout. The calculative results show an elevation in the performance values as the ADC evaporator temperature rises. The explanatory of this increase is that as the ADC evaporator temperature increases, the ADC cooling load decreases (Fig. 3), and lower heat input is required to the thermal compressor. On the contrary, as the ADC cooling load decreases, the VCC cooling load increases (as the total heat load is kept constant at 10 kW in the two evaporators); thus, more electrical energy is required to drive the VCC system. By implementing these quantities in Eq. (35), the results appear as illustrated in Fig. 6(b). The highest performance reached 0.354 for silica gel-LiCl at the highest ADC evaporator temperature considered in the current paper. In contrast, the lowest performance values are reported using RD silica gel 2060 as it requires higher heat rates $\dot{Q}_{heat,ADC}$ as illustrated in Fig. 4. Besides that, the increasing ratios in the overall combined system performance in the serial connected evaporators configuration by increasing the ADC temperature from 10 °C to 20 °C are 8.4%, 9.1%, and 7.3% for RD silica gel, RD silica gel 2060, and silica gel-LiCl, respectively.

Fig. 7(a) illustrates the overall system performance of the ADC-VCC combined cooling system according to the type A and type B configurations shown in (Fig. 1a and b) at three different cycle times (1100 [s], 900[s], and 700[s]) and various ADC evaporator temperature $T_{eva,ADC}$. The results shown in Fig. 7 were calculated on the ADC-VCC combined cooling system employing RD silica gel/water in the ADC unit and R152A refrigerant in the vapor compression chiller. The results clarify that lowering the cycle time decreases the overall system performance in both configurations considered (a and b). Reducing the cycle time leads to more amount of heat ($\dot{Q}_{heat,ADC}$) needed to the adsorption system; thus, lower performance in the whole combined system. Where decreasing the cycle time from 1100s to 700s results in decreasing the coefficient of performance from (0.33–0.284) for series connection at ($T_{eva,ADC} = 10$ °C) which is about 14%. The highest performance values were obtained when using 1100 [s] as an adsorption cycle time. While the lowest performance values were reported at 700 [s] as an adsorption cycle time. It should be mentioned that determining the cycle time for the adsorption cooling cycle is essential where the time should be sufficient to successfully accomplish the desorption and adsorption processes. Fig. 7(a) also illustrates the effect of using different evaporator temperature $T_{eva,ADC}$ from (10 °C–20 °C), which was previously explained in Fig. 6. The highest values were obtained when considering 1100 [s] as a cycle time reached up to 0.35 at ($T_{eva,ADC} = 20$ °C) while the lowest system performance values were provided when considering 700 [s] as adsorption cycle time reached 0.27 at ($T_{eva,ADC} = 10$ °C) for serial connected evaporators (type B) configuration.

Fig. 7(b) exhibits the results of the overall system performance $COP_{EXE,H}$ at different ambient temperatures and various ADC temperatures for type A and type B configurations, as shown in Fig. 1. The results illustrated in Fig. 7(b) are the results of employing RD silica gel/water as a working pair in adsorption chiller and R152A refrigerant in vapor compression chiller. The results indicate that increasing the ambient temperature leads to an elevation in the overall performance $COP_{EXE,H}$ reached 0.35 at the highest ambient temperature considered in this study. The exergy values of the heat quantities for the cascaded (type A) and the serial connected evaporators (type B) configurations ($\dot{Q}_{eva,VCC}$ $\dot{Q}_{eva,ADC}$, and $\dot{Q}_{heat,ADC}$) are a function of ambient temperature T_{amb}. Thus, modifying the ambient temperature will certainly affect the overall system performance, according to Eq. (34) and Eq. (35). Additionally, rising the ADC evaporator temperature leads to a decline in the system performance that operates in the type A layout and an increase in the system performance that works in the type B layout, which was previously discussed in Fig. 6. The results also reveal that both system connections (type A and type B) provide the same overall system performance if they operate at a specific ADC evaporator temperature.



(a) (b)

Fig. 7. Comparisons of $COP_{EXE,H}$ with respect to ADC evaporator temperature between the type A and type B configurations at different adsorption (a) cycle times and (b) ambient temperatures.

For instance, at ($T_{eva,ADC} = 15\ ^{\circ}C$) both combined systems (type A and type B) provide ($COP_{EXE,H} = 0.209$) if they are operated at ($T_{amb} = 28\ ^{\circ}C$). It is noteworthy to mention that the same behavior was observed during the calculations if the RD silica gel 2060 or silica gel-LiCl were employed. The results reveal that the overall system performance in the cascaded configuration (type A) increases by 52.3% and 49% at 28 °C and 40 °C, respectively. While the overall system performance in the type B configuration increases by 63.7% and 43.2% at 28 °C and 40 °C, respectively.

Fig. 8 shows the relation between the adsorbent amount and the adsorbent types used in this investigation at different ADC cooling loads ranged from 5 kW to 15 kW. It is noteworthy to indicate that the $T_{eva,ADC}$ is kept constant in this evaluation at 15 °C. It can be noticed from the results that as the cooling load increases, the COP_{ADC} also increases. Even though increasing the $\dot{Q}_{eva,ADC}$ leads to a rise in the heat input to the thermal compressor (at constant $T_{eva,ADC}$), increasing the evaporator heat has more impact on raising the ADC performance values than increasing the heat input. It is also evident from the results that employing a lower amount of adsorbent mass provides higher system performance values. However, the amount of adsorbent should be carefully determined as it affects the amount of the adsorbate (refrigerant) in the ADC chiller, which should be sufficient to accomplish the evaporation required in the ADC evaporator. Fig. 8 also reveals that the highest and lowest values COP_{ADC} were obtained using 20 kg of the silica gel-LiCl and 40 kg of RD silica gel 2060, respectively, within the range considered in this evaluation. The highest COP_{ADC}value reached 0.71 at ($\dot{Q}_{eva,ADC} =$ 15 kW). In contrast, the lowest COP_{ADC} value reached up to 0.39 at ($\dot{Q}_{eva,ADC} = 5$ kW).

Fig. 9 presents the results of the ADC system performance of the proposed combined cooling system when using the different adsorbents considered with the two different layouts (type A and type B). The comparison has been made at different ADC evaporator temperatures ranged from 10 °C to 20 °C. It is evident from Fig. 9 that there is a slight elevation in the COP_{ADC} as the $T_{eva,ADC}$ increases for cascaded (type A) configuration reached up to 0.584 by using composite adsorbent in the thermal compressor. The reason for this resulting is that as the evaporator temperature increases, which is also related to the VCC condenser temperature ($\Delta T = 5\ ^{\circ}C$), the ADC evaporator heat ($\dot{Q}_{eva.ADC,a}$) also increases, which leads to slight increases in the COP_{ADC}. In contrast, in the serial connected evaporators (type B) arrangement, as the ADC evaporator temperature increases, the outlet temperature of the secondary working fluid also increases ($T_{II} = T_{eva,ADC} + 2$), which leads to lower heat absorbed from the second working fluid ($\dot{Q}_{eva.ADC,b}$). As a result, lower ADC performance values COP_{ADC} were obtained. It is also apparent from the results that silica gel-LiCl provides the highest performance values for both configurations considered in this research. The results reveal that increasing the ADC evaporator temperature from 10 °C to 20 °C leads to an increase in the ADC performance by nearly 11.2% for all the adsorbents considered in the cascaded configuration (type A). At the same time, there is a reduction in the ADC performance 51.6%, 51%, and 50.9% for RD silica gel, RD silica gel 2060, and RD silica gel LiCl, respectively, in the serial connected evaporators layout (type B).

Fig. 10 shows the comparisons between the coefficient of performance for the vapor compression chiller integrated with the adsorption chiller according to the two layouts (type A and type B) considered in this paper. It is essential to mention that the temperature difference between the VCC condenser and ADC evaporator is kept constant at ($\Delta T = 5\ ^{\circ}C$) for the cascaded configuration (Fig. 1a). Fig. 10 reveals that as the ADC evaporator temperature ($T_{eva,ADC}$) increases within the range considered, the VCC coefficient of performance (COP_{VCC}) decreases by 35.8%. Elevating the ADC evaporator temperature drives to a rise in the VCC condenser temperature; thus, more electrical power is needed for the vapor compression chiller; therefore, lower VCC performance values at constant cooling load (10 kW). On the contrary, the coefficient of performance values of vapor compression chiller linked with adsorption chiller in the serial connected evaporators configuration (Fig. 1b) almost remain constant by increasing the ADC evaporator temperature $T_{eva,ADC}$. As previously mentioned, the connection between the two chillers considered occurs in the secondary fluid that connects the ADC evaporator with the VCC evaporator. Therefore, increasing the ADC evaporator temperature leads to lower ADC

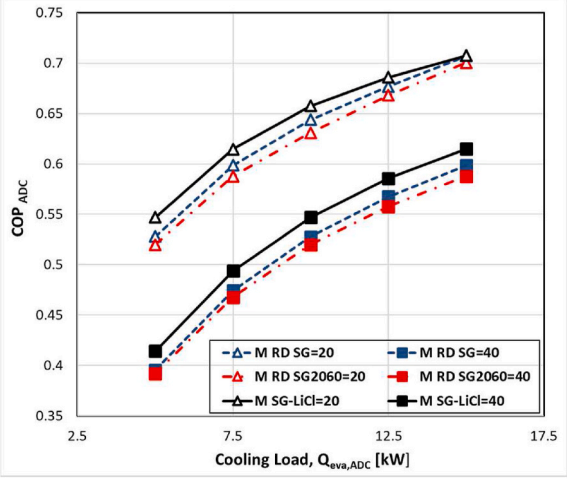


Fig. 8. Comparisons of ADC system performance with respect to different cooling loads $\dot{Q}_{eva,VCC}$ using the three adsorbents considered and two adsorbent mass values.

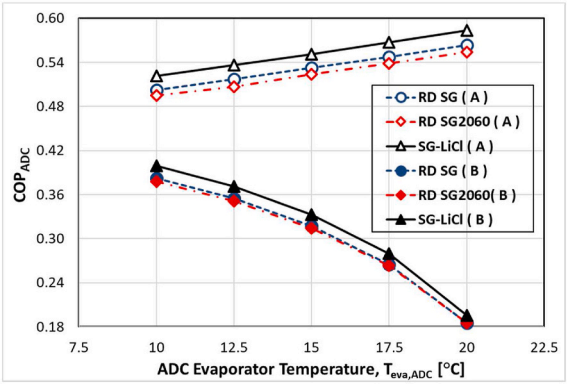


Fig. 9. Comparisons of COP_{ADC} with respect to ADC evaporator temperature using different adsorbents in ADC for (type A and type B) configurations.

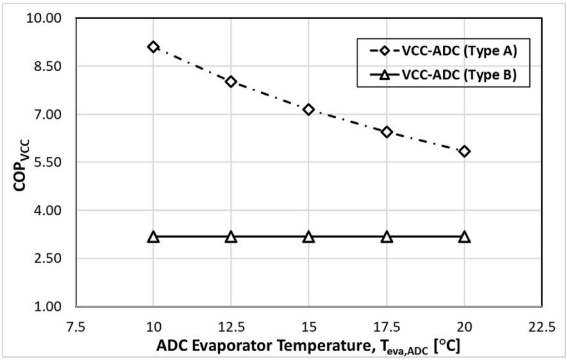


Fig. 10. Comparisons of COP_{VCC} with respect to ADC evaporator temperature using the two different layouts (type A and type B).

cooling load absorbed ($\dot{Q}_{eva,ADC,b}$) in the ADC evaporator and higher VCC cooling load absorbed ($\dot{Q}_{eva,VCC,b}$) in the VCC evaporator. However, the evaporator and condenser temperatures are kept constant in the vapor compression chiller, and the VCC cooling load is only modified at different ADC evaporator temperatures; thus, increasing the VCC cooling loads ($\dot{Q}_{eva,VCC}$) due to the increase in the ADC evaporator temperature drives to a rise in the electrical power consumed by the mechanical compressor in the vapor compression chiller. Therefore, the VCC coefficient of performance remains nearly constant in the type B configuration and lower than the coefficient of performance in the cascaded configuration (type A). The highest VCC coefficient of performance reached to 9.1 at ($T_{eva,ADC}$ = 10 °C). The computed results also reveal that if the vapor compression chiller operates alone (without adsorption chiller) at the same operating conditions ($T_{eva,VCC}$ = -5 °C, $T_{cond,VCC}$ = 45 °C, $\dot{Q}_{eva,VCC}$ = 10 kW) the VCC coefficient of performance is 3.18 by employing R152A, and the electrical power is higher than the two layouts considered in this paper. This means that the vapor compression chiller operates more effectively with a lower VCC system size if it is combined with the adsorption chiller at the same operating conditions.

Table 4 shows the comparisons of the variation of electrical energy saving ratio (EESR) with respect to the ADC evaporator temperatures for both configurations (type A and type B) as if the VCC system operates alone at the same running conditions. The results illustrate that increasing the ADC evaporator temperature results in a gradual decrease in the EESR in the cascaded configuration (type A). In contrast, increasing the same parameter leads to a sharp reduction in the EESR values for the serial connected evaporators configuration (type B). The difference between these two behaviors is that in type A, increasing the ADC temperature leads to an increase in the VCC condenser ($\Delta T = 5$ °C). While increasing the ADC evaporator temperature in type B leads to a higher cooling load in the VCC evaporator (Fig. 3) and higher electrical energy consumption. The highest EESR values reached up to 65% for the series linkage and 59% for the type B at ($T_{eva,ADC}$ = 10°C). In contrast, the lowest EESR values reached up to 46% for the cascaded configuration (type A) and 13% for the type B layout at ($T_{eva,ADC}$ = 20°C).

Table 5 reports the performance ratio values of the ADC and VCC of the hybrid cooling system compared with the performance of the ADC and VCC chillers as if they operate alone under the same running conditions considering the RD silica gel in the thermal compressor with respect to the ADC evaporator temperature ranging from 10 °C to 20 °C.

Table 6 shows the comparisons of the effectiveness of the ADC and VCC evaporators (ε_{eva}) with respect to the ADC evaporator temperatures according to the type B layout. It is clear from the results that as the ADC evaporator temperature increases, the ADC evaporator effectiveness ($\varepsilon_{eva,ADC,b}$) decreases due to lower cooling load absorbed through the ADC evaporator (Fig. 3). The highest ADC evaporator effectiveness value reached 0.867. In contrast, increasing the ADC evaporator temperature results in an increase in the

Table 4
Electrical energy saving ratio (EESR) with respect to the ADC evaporator temperatures for type A and type B configurations.

$T_{eva,ADC}$	Electrical energy saving ratio (EESR)	
	Type A	Type B
10	65%	59%
12.5	60%	48%
15	55%	35%
17.5	50%	25%
20	46%	13%

Table 5
Performance ratios of the ADC and VCC chillers.

$T_{eva,ADC}$	Type A		Type B	
	PR_{VCC}	PR_{ADC}	PR_{VCC}	PR_{ADC}
10	2.861	1.038	1.00	0.79
12.5	2.52	1.041	1.00	0.74
15	2.246	1.043	1.00	0.623
17.5	2.023	1.045	1.00	0.506
20	1.835	1.046	1.00	0.344

effectiveness values of the VCC evaporator $\varepsilon_{eva,VCC,b}$ due to higher cooling load is absorbed in the VCC evaporator. The highest value observed is 0.824. It is noteworthy to mention that the VCC evaporator effectiveness is $\varepsilon_{eva,VCC,a} = 0.846$ for the type A configuration as the cooling load is 10 kW, and the inlet and outlet temperatures of the secondary fluid are 25 °C and 3 °C, respectively.

8. Conclusions

The current article concentrates on a comparative appraisal of a cooling system comprised of integrated two cooling technologies, namely the adsorption cooling system (ADC) and conventional vapor mechanical cooling system (VCC). The adsorption chiller has a thermal compressor (two adsorption beds) with three different types of adsorbent separately (RD silica gel, RD silica gel 2060, and silica gel-LiCl) and water as the adsorbate. The vapor compression chiller uses R152A as a refrigerant. These different ADC adsorbents with two different system configurations (cascaded and serial connected evaporators configurations) were studied and discussed at different ADC evaporator temperatures ranged from 10 °C to 20 °C. The computed results reveal the following conclusions:

- Among the all considered adsorbents, silica gel-LiCl gives the highest overall system performance $COP_{EXE,H}$ values reached up to 0.354 within the operating conditions utilized in this study. In contrast, RD silica gel 2060 provides the lowest performance values, reached up to 0.3 at the same working conditions considered in this article.
- The overall system performance $COP_{EXE,H}$ increases as the ADC evaporator temperature increases in the serial connected evaporators configuration. While it decreases in the cascaded configuration. Additionally, the reduction ratios in the overall combined system performance $COP_{EXE,H}$ by increasing the ADC temperature from 10 °C to 20 °C in the cascaded configuration are almost 9.70%, 9.40%, and 9.74% for RD silica gel, RD silica gel 2060, silica gel-LiCl, respectively. In the contrary, the increasing ratios in $COP_{EXE,H}$ in the serial connected evaporators configuration within the same ADC evaporator temperature range are 8.4%, 9.1%, and 7.3% for RD silica gel, RD silica gel 2060, and silica gel-LiCl, respectively.
- Among the three considered adsorbents, silica gel-LiCl gives the highest ADC performance COP_{ADC} values reached up to 0.584 within the operating conditions utilized in this study. The highest ADC performance values were also obtained using the cascaded configuration compared to the serial connected evaporators configuration. The results also accentuated that elevating the ADC

Table 6
Comparisons of evaporator effectiveness (ε_{eva}) of ADC and VCC chillers with respect to the ADC evaporator temperatures for the serial connected evaporators configuration (type B).

$T_{eva,ADC}$	ε_{eva}	
	ADC	VCC
10	0.87	0.67
12.5	0.83	0.73
15	0.80	0.77
17.5	0.73	0.80
20	0.60	0.82

evaporator temperature leads to a slight increase in the ADC coefficient of performance in a cascaded connection with the VCC unit. In contrast, it reduces the ADC coefficient of performance in the serial connected evaporators configuration. Increasing the ADC evaporator temperature from 10 °C to 20 °C leads to an increase in the ADC performance by nearly 11.2% for all the adsorbents considered in the cascaded connection. At the same time, there is a reduction in the ADC performance by 51.6%, 51, 50.9% for RD silica gel, RD silica gel 2060, and RD silica gel LiCl, respectively, in the serial connected evaporators configuration.

- The results demonstrated that the adsorption cycle time affects the overall combined cooling system $COP_{EXE,H}$. The cycle time should be sufficient to complete the adsorption/desorption process successfully. The higher the adsorption cycle time, the better the overall system performance. Increasing the cycle time from 700s to 1100s results in increasing the coefficient of performance from (0.284–0.33) for series connection at ($T_{eva,ADC} = 10$ °C) which is about 16.2%.
- The current results also reveal the relationship between the ADC cooling load and the adsorbent mass required to design the ADC chiller. Lower mass gives higher COP_{ADC} values at the same $\dot{Q}_{eva,VCC}$. In contrast, higher $\dot{Q}_{eva,VCC}$ values result in higher COP_{ADC} values at the same amount of adsorbents. Additionally, among all the adsorbents considered, the composite adsorbent (silica gel-LiCl) gives the highest COP_{ADC} values at the same $\dot{Q}_{eva,VCC}$ reached up to 0.71 at the higher $\dot{Q}_{eva,VCC}$ value considered in this paper.
- The evaluation of vapor compression chiller performance in the combined chiller with respect to ADC evaporator temperature illustrates that the serial connected evaporators configuration provides lower system performance COP_{VCC} values than the cascaded connection. However, VCC chiller integrated with the ADC chiller generally operates more productive than working alone under the same operating conditions. Additionally, the highest VCC performance ratio reached up to 2.86 on the cascaded configuration according to different ADC evaporator temperatures. In contrast, the ADC performance ratio is close to one in cascaded connection and lower than one in serial connected evaporators configuration.
- The appraisal of using the proposed combined cooling system at different ambient temperature conditions reveals that increasing the ambient temperature rises the overall system performance $COP_{EXE,H}$ for both types of connections reached up to 0.35 for serial connected evaporators configuration at the highest ambient temperature considered in this paper (40 °C). Furthermore, there is a specific value of the ADC evaporator temperature at which both systems supply that same overall system performance value. The results also show that the overall system performance in the cascaded connection increases by 52.3% and 49% at 28 °C and 40 °C, respectively. In comparison, it increases by 63.7% and 43.2% at 28 °C and 40 °C, respectively, in the serial connected evaporators configuration.

Author statement

Conceptualization, M.K and M.A.; methodology, M.K; numerical simulation, M.K and M.A.; validation, M.K and M.A.; investigation, M.K and M.A.; data curation, M.K and M.A.; writing—original draft preparation, M.K and M.A.; writing—review and editing, M.K.; supervision, M.K.

Declaration of competing interest

The authors declare that they have no known competing financial interests or personal relationships that could have appeared to influence the work reported in this paper.

References

[1] A. Allouhi, T. Kousksou, A. Jamil, T. El Rhafiki, Y. Mourad, Y. Zeraouli, Optimal working pairs for solar adsorption cooling applications, Energy 79 (2015) 235–247, https://doi.org/10.1016/j.energy.2014.11.010. C.
[2] A.N. Shmroukh, A.H.H. Ali, S. Ookawara, Adsorption working pairs for adsorption cooling chillers: a review based on adsorption capacity and environmental impact, Renew. Sustain. Energy Rev. 50 (2015) 445–456, https://doi.org/10.1016/j.rser.2015.05.035.
[3] P. Kumar, A. Sharma, Experimental analysis of mechanical and adsorption hybrid refrigeration with CO2 as refrigerant and activated carbon as absorbent, Int. J. Eng. Res. Technol. 3 (8) (2014) 883–890.
[4] A.F. Altun, M. Kılıç, An investigation of the ammonia adsorption performance on different adsorbents for cooling applications, Bulg. Chem. Commun. 50 (January 2019) (2018) 45–52.
[5] M. Kılıç, Comparative performance analysis of a two-bed adsorption cooling system with adsorption of different adsorbates on silica-gel, Bulg. Chem. Commun. 50 (2018) 102–110. G.
[6] B.B. Saha, A. Chakraborty, S. Koyama, Y.I. Aristov, A new generation cooling device employing CaCl2-in-silica gel-water system, Int. J. Heat Mass Tran. 52 (1–2) (2009) 516–524, https://doi.org/10.1016/j.ijheatmasstransfer.2008.06.018.
[7] X. Li, H. Li, S. Huo, Z. Li, Dynamics and isotherms of water vapor sorption on mesoporous silica gels modified by different salts, Kinet. Catal. 51 (5) (2010) 754–761, https://doi.org/10.1134/S0023158410050186.
[8] L.X. Gong, R.Z. Wang, Z.Z. Xia, C.J. Chen, Design and performance prediction of a new generation adsorption chiller using composite adsorbent, Energy Convers. Manag. 52 (6) (2011) 2345–2350, https://doi.org/10.1016/j.enconman.2010.12.036.
[9] S. Vasta, V. Palomba, D. La Rosa, W. Mittelbach, Adsorption-compression cascade cycles: an experimental study, Energy Convers. Manag. 156 (December 2017) (2018) 365–375, https://doi.org/10.1016/j.enconman.2017.11.061.
[10] K. Uddin, T. Miyazaki, S. Koyama, B.B. Saha, Performance investigation of adsorption–compression hybrid refrigeration systems, Int. J. Air-Conditioning Refrig. 21 (2013) 1350024, https://doi.org/10.1142/s2010132513500247, 04.
[11] V. Palomba, G.E. Dino, A. Frazzica, Coupling sorption and compression chillers in hybrid cascade layout for efficient exploitation of renewables: sizing, design and optimization, Renew. Energy 154 (2020) 11–28, https://doi.org/10.1016/j.renene.2020.02.113.
[12] G. Lychnos, Z. Tamainot-Telto, Performance of hybrid refrigeration system using ammonia, Appl. Therm. Eng. 62 (2) (2014) 560–565, https://doi.org/10.1016/j.applthermaleng.2013.10.013.
[13] G. Lychnos, Z. Tamainot-Telto, Prototype of hybrid refrigeration system using refrigerant R723, Appl. Therm. Eng. 134 (2018) 95–106, https://doi.org/10.1016/j.applthermaleng.2017.12.103.

[14] M. Kilic, M. Anjrini, Comparative performance analysis of a combined cooling system with mechanical and adsorption cycles, Energy Convers. Manag. 221 (2020) 113208, https://doi.org/10.1016/j.enconman.2020.113208. July.
[15] V. Jain, G. Sachdeva, S.S. Kachhwaha, Energy, exergy, economic and environmental (4E) analyses based comparative performance study and optimization of vapor compression-absorption integrated refrigeration system, Energy 91 (2015) 816–832, https://doi.org/10.1016/j.energy.2015.08.041.
[16] Z. Seyfouri, M. Ameri, Analysis of integrated compression-absorption refrigeration systems powered by a microturbine, Int. J. Refrig. 35 (6) (2012) 1639–1646, https://doi.org/10.1016/j.ijrefrig.2012.04.010.
[17] S.M. Hojjat Mohammadi, M. Ameri, Energy and exergy comparison of a cascade air conditioning system using different cooling strategies, Int. J. Refrig. 41 (2014) 14–26, https://doi.org/10.1016/j.ijrefrig.2013.06.015.
[18] P.J. Vodianitskaia, J.J. Soares, H. Melo, J.M. Gurgel, Experimental chiller with silica gel: adsorption kinetics analysis and performance evaluation, Energy Convers. Manag. 132 (2017) 172–179, https://doi.org/10.1016/j.enconman.2016.11.028.
[19] A. Freni, G. Maggio, A. Sapienza, A. Frazzica, G. Restuccia, S. Vasta, Comparative analysis of promising adsorbent/adsorbate pairs for adsorptive heat pumping, air conditioning and refrigeration, Appl. Therm. Eng. 104 (2016) 85–95, https://doi.org/10.1016/j.applthermaleng.2016.05.036.
[20] A. Sharafian, M. Bahrami, Critical analysis of thermodynamic cycle modeling of adsorption cooling systems for light-duty vehicle air conditioning applications, Renew. Sustain. Energy Rev. 48 (2015) 857–869, https://doi.org/10.1016/j.rser.2015.04.055.
[21] A.A. Askalany, M. Salem, I.M. Ismael, A.H.H. Ali, M.G. Morsy, B.B. Saha, An overview on adsorption pairs for cooling, Renew. Sustain. Energy Rev. 19 (2013) 565–572, https://doi.org/10.1016/j.rser.2012.11.037.
[22] B.B. Saha, S. Koyama, I.I. El-Sharkawy, K. Habib, K. Srinivasan, P. Dutta, Evaluation of adsorption parameters and heats of adsorption through desorption measurements, J. Chem. Eng. Data 52 (6) (2007) 2419–2424, https://doi.org/10.1021/je700369j.
[23] R.H. Mohammed, O. Mesalhy, M.L. Elsayed, S. Hou, M. Su, L.C. Chow, Physical properties and adsorption kinetics of silica-gel/water for adsorption chillers, Appl. Therm. Eng. 137 (October 2017) (2018) 368–376, https://doi.org/10.1016/j.applthermaleng.2018.03.088.
[24] H.T. Chua, K.C. Ng, A. Malek, T. Kashiwagi, A. Akisawa, B.B. Saha, Modeling the performance of two-bed, silica gel-water adsorption chillers, Int. J. Refrig. 22 (3) (1999) 194–204, https://doi.org/10.1016/S0140-7007(98)00063-2.
[25] I.I. El-Sharkawy, K. Kuwahara, B.B. Saha, S. Koyama, K.C. Ng, Experimental investigation of activated carbon fibers/ethanol pairs for adsorption cooling system application, Appl. Therm. Eng. 26 (8–9) (2006) 859–865, https://doi.org/10.1016/j.applthermaleng.2005.10.010.
[26] I.H. Bell, J. Wronski, S. Quoilin, V. Lemort, Pure and pseudo-pure fluid thermophysical property evaluation and the open-source thermophysical property library coolprop, Ind. Eng. Chem. Res. 53 (6) (2014) 2498–2508, https://doi.org/10.1021/ie4033999.
[27] J. Di, J.Y. Wu, Z.Z. Xia, R.Z. Wang, "Theoretical and experimental study on characteristics of a novel silica gel e water chiller under the conditions of variable heat source temperature ' orique et expe ' rimentale sur les caracte ' ristiques d ' un Etude the refroidisseur innovant fonctionn 30 (2007), https://doi.org/10.1016/j.ijrefrig.2006.07.022.
[28] B.O. Bolaji, Z. Huan, Ozone depletion and global warming : case for the use of natural refrigerant – a review, Renew. Sustain. Energy Rev. 18 (2013) 49–54, https://doi.org/10.1016/j.rser.2012.10.008.